Nonlinear Dynamics (2005) 39: 235–258

Double Hopf Bifurcation Analysis Using Frequency Domain Methods

GRISELDA R. ITOVICH[1] and JORGE L. MOIOLA[2,*]

[1]*Departamento de Matemática, FAEA, Universidad Nacional del Comahue, Neuquén, Q8300BCX, Argentina;* [2]*Departamento de Ingeniería Eléctrica y de Computadoras, Universidad Nacional del Sur, Bahía Blanca, B8000CPB, Argentina;*
[*]*Author for correspondence (e-mail: jmoiola@criba.edu.ar; fax: +54-291-4595154)*

(Received: 7 August 2003; accepted: 9 July 2004)

Abstract. The dynamic behavior close to a non-resonant double Hopf bifurcation is analyzed via a frequency-domain technique. Approximate expressions of the periodic solutions are computed using the higher order harmonic balance method while their accuracy and stability have been evaluated through the calculation of the multipliers of the monodromy matrix. Furthermore, the detection of secondary Hopf or torus bifurcations (Neimark–Sacker bifurcation for maps) close to the analyzed singularity has been obtained for a coupled electrical oscillatory circuit. Then, quasi-periodic solutions are likely to exist in certain regions of the parameter space. Extending this analysis to the unfolding of the 1:1 resonant double Hopf bifurcation, cyclic fold and torus bifurcations have also been detected in a controlled oscillatory coupled electrical circuit. The comparison of the results obtained with the suggested technique, and with continuation software packages, has been included.

Key words: double Hopf bifurcation, harmonic balance, limit cycles, Neimark–Sacker bifurcation

1. Introduction

The qualitative changes of the solutions in a multiparameter dynamical system of nonlinear differential equations are studied through bifurcation theory. This subject is usually considered in a state-variable formulation (time-domain method) but there exists another approach that comes from the theory of feedback systems known as frequency-domain method which is familiar to control engineers and then of practical interest in the field of control and anti-control of bifurcations. Using this perspective whose starting point is the application of the Laplace transform, it is possible to consider the bifurcation problems in differential equations through certain loci, called Nyquist diagrams, in the complex plane. Regarding the dynamic bifurcations which involve the appearance or disappearance of limit cycles, certain family of degeneracies has been analyzed. More specifically, the subject of this paper comprises when one of the hypotheses of the Poincaré–Andronov–Hopf theorem [1] fails: the linearized system evaluated at the equilibrium has exactly two pairs of purely imaginary eigenvalues: $\pm i\omega_1$, $\pm i\omega_2$ (ω_1/ω_2 is an irrational number) instead of a single pair of the classical theorem. This singularity, known as the non-resonant double Hopf bifurcation, is locally described through the changes of two unfolding parameters. Using the frequency domain approach, it has been established that two Hopf curves, each one associated with a specific value of frequency (ω_1 and ω_2, respectively), cross the referred singularity in the parameter space. This type of singularity is directly related with the phenomena of secondary Hopf bifurcations, leading to the existence of quasi-periodic solutions (2-D torus with frequencies ω_1 and ω_2, as shown in [2, 3] and [4]). Using Floquet theory and higher-order harmonic balance, the problem of detecting the bifurcation of cycles has been developed. In this case, a semi-analytical approximation of the periodic solution close to criticality is obtained using harmonic balance of eighth-order which meant

that the periodic solution is expanded up to eight harmonics, and the changes of stability have been evaluated through the computation of the eigenvalues of the monodromy matrix. Then, the detection of Neimark–Sacker bifurcations (or torus) bifurcations is developed using the proposed method. All the numerical results have been contrasted to those obtained with LOCBIF [5]. It is known that the analyzed singularity can be found in the unfolding of a 1:1 resonant double Hopf bifurcation [6]. Henceforth, some related outcomes in the frequency domain setting are also shown.

One important research line for the analysis of non-resonant double Hopf bifurcation is concentrated in the application of perturbation techniques [7, 8] for the determination of normal forms [9] which are finally used for the stability analysis, nowadays supported by the power of computing algebraic systems as Mathematica or Maple (see [4]). In this work and with the same proposal, the formulation is now based on feedback systems theory, which employs harmonic balance approximation techniques to build the periodic solutions and solves the stability problems through the determination of characteristic multipliers [10]. The quasi-periodic motion can also be recognized as a recurrent but nonrepetitive oscillatory equilibrium [11]. The number of fundamental frequencies involved in its power spectrum might be called degree of quasi-periodicity. In this sense, it is known that quasi-periodicity of degree greater than two is of sporadic appearance. However, some theoretical results show that any n-D torus attractor, with $n = 3, 4$, can be slightly perturbed into chaos and in this regard, a related problem of multiple input excitation frequencies and the determination of the stability of a quasi-periodic solution has been extensively documented [12]. Returning to the phenomena of double Hopf bifurcations, some interesting works on applications in aeroelastic oscillators [13, 14] and various problems in wind and mechanical engineering [15, 16] were developed.

In this work, Section 2 is an exposition of preliminary results about bifurcations in a nonlinear system of differential equations in the frequency domain, with stress in the cases known as non-resonant and 1:1 resonant double Hopf bifurcation. Following this point of view, in Section 3, some aspects regarding the version of Poincaré–Andronov–Hopf theorem and the associated graphical method for obtaining the approximate expression of the periodic solution, which employs harmonic balance of high order, are expounded. In Section 4, some basic notions of Floquet multipliers are stated. The obtained results, particularly those for the determination of the secondary Hopf bifurcation curve, are shown in Section 5. Finally, the attained conclusions are presented and some research lines to explore in the future are mentioned in Section 6.

2. Formulation

Let us consider a nonlinear system like

$$\dot{x} = f(x; \eta), \tag{1}$$

where $x \in R^n$, $\dot{x} = \frac{dx}{dt}$ and $\eta \in R^m$, with an equilibrium at the origin. For simplicity, assume that $\eta = \eta_1 \in R^1$ is the main bifurcation parameter for the case of Hopf bifurcation and progressed in order to describe later the double Hopf case with two parameters, namely $\eta = (\eta_1, \eta_2)$. This system can be seen as a feedback realization considering $u \in R^p$ the control input and $y \in R^l$ the system output

$$\begin{aligned} \dot{x} &= Ax + Bu, \\ y &= -Cx, \\ u &= g(y; \eta_1), \end{aligned} \tag{2}$$

where $A = A(\eta_1)$ is an $n \times n$ matrix, chosen for convenience (invertible and stable for each assignment of the parameter η_1), $B = B(\eta_1)$ and $C = C(\eta_1)$ are matrices of order $n \times p$ and $l \times n$, respectively, and g is a nonlinear vectorial function in R^p, $g \in C^{(2q+2)}$ in both variables y and η_1, where $2q$ is the number of harmonics that will be involved in the expression of the periodic solution.

Supposing a zero initial condition in (2), the equilibrium points in the frequency domain are the solutions of the following equation:

$$\tilde{y}(t; \eta_1) = -G(0; \eta_1) g(\tilde{y}(t; \eta_1); \eta_1), \tag{3}$$

where $G(s; \eta_1) = C(\eta_1)(sI - A(\eta_1))^{-1} B(\eta_1)$ is the standard transfer matrix of the linear part of (2).

Linearizing (2) about the equilibrium $\tilde{y} = \tilde{y}(t; \eta_1)$, the resulting system has $J(\eta_1) = D_1 g(\tilde{y}; \eta_1) = \frac{\partial g}{\partial y}|_{y=\tilde{y}}$ as its Jacobian. Thus, the next result can be applied [17].

Lemma 1. *If* $\mathrm{i}\omega_0$ *is an eigenvalue of the Jacobian of the nonlinear system* (2), *in the time domain*, *when* $\eta_1 = \eta_1^*$, *then the corresponding eigenvalue of the constant matrix* $G(\mathrm{i}\omega_0; \eta_1^*) J(\eta_1^*)$ *in the frequency domain must assume the value* $(-1 + \mathrm{i}0)$.

Following the frequency domain approach, the characteristic polynomial of the matrix $G(s; \eta_1) J(\eta_1)$, namely

$$h = h(\lambda, s; \eta_1) = \det(\lambda I - G(s; \eta_1) J(\eta_1)), \tag{4}$$

carries on the stability of the equilibrium point, via the application of the generalized Nyquist stability criterion. Due to the previous lemma, it is straightforward that:

$$h(-1, \mathrm{i}\omega_0; \eta_1^*) = \det(-I - G(\mathrm{i}\omega_0; \eta_1^*) J(\eta_1^*)) = 0, \tag{5}$$

and therefore

$$\begin{cases} F_1(\omega, \eta_1) = \mathrm{Re}\{h(-1, \mathrm{i}\omega; \eta_1)\} = 0, \\ F_2(\omega, \eta_1) = \mathrm{Im}\{h(-1, \mathrm{i}\omega; \eta_1)\} = 0, \end{cases} \tag{6}$$

for $\omega = \omega_0$ and $\eta_1 = \eta_1^*$, where $\mathrm{Re}(\cdot)$ and $\mathrm{Im}(\cdot)$ represent the real and imaginary parts of a complex number, respectively. Naturally, system (6) gives a necessary condition to have a dynamic or Hopf bifurcation at the point (ω_0, η_1^*), if $\omega_0 \neq 0$.

Using the functions F_1, F_2 and their partial derivatives, it can be established some defining and non-degeneracy conditions for certain types of static and dynamic bifurcations [18,19]. Particularly, it will be analyzed one family of degeneracies that arises when one of the hypotheses of Poincaré–Andronov–Hopf theorem [1] fails, more precisely, this situation appears when the Jacobian of the system evaluated at equilibrium has two pairs of purely imaginary eigenvalues $\pm\mathrm{i}\omega_1, \pm\mathrm{i}\omega_2$ where (ω_1/ω_2) is an irrational number. It is known that this singularity can be locally described using two auxiliary parameters, that will be noted as $\eta = (\eta_1, \eta_2)$. A direct result has been stated in [18] and is adapted here with minor changes in notation.

Proposition 1. *A necessary condition for the existence of a non-resonant double Hopf bifurcation at* $\eta^* = (\eta_1^*, \eta_2^*)$ *is*

$$F_1(\omega_i, (\eta_1^*, \eta_2^*)) = F_2(\omega_i, (\eta_1^*, \eta_2^*)) = 0, \quad i = 1, 2, \tag{7}$$

where (ω_1/ω_2) *is an irrational number.*

Related with this type of bifurcation, it is known that two branches of the Hopf bifurcation curve intersect each other at the referred singularity [2, 3]. In the frequency domain setting, it follows the next proposition.

Proposition 2. *If there is a non-resonant double Hopf bifurcation at* $\eta^* = (\eta_1^*, \eta_2^*)$, *with frequencies* ω_i *and*

$$\left| \frac{\partial(F_1, F_2)}{\partial(\eta_1, \eta_2)} \bigg|_{(\omega_i, \eta^*)} \right| \neq 0, \quad i = 1, 2, \tag{8}$$

then two branches of the Hopf bifurcation curve cross each other at criticality, with the following tangents vectors:

$$t_i = \left(\left| \frac{\partial(F_1, F_2)}{\partial(\omega, \eta_2)} \bigg|_{(\omega_i, \eta^*)} \right|, -\left| \frac{\partial(F_1, F_2)}{\partial(\omega, \eta_1)} \bigg|_{(\omega_i, \eta^*)} \right| \right), \quad i = 1, 2. \tag{9}$$

Proof. This result is a direct consequence of the application of the Implicit Function Theorem to the system pointed out in Proposition 1. □

Observation 1: The hypothesis about the Jacobian determinant is not restrictive if one takes into account that a non-resonant double Hopf bifurcation always can be thought close to a 1:1 resonant one, i.e. $\omega_1 = \omega_2 \neq 0$ [6], where such condition is supposed to be satisfied (see Theorem 1).

Observation 2: Approximate expressions of higher order for these Hopf bifurcation curves can be obtained through the functions F_1, F_2 and its derivatives, using Taylor expansions. Particularly, Proposition 2 yields linear approximations of them.

Observation 3: A change of stability in the crossing of the aforementioned two branches has been stated in [2, 3].

Connected with the 1:1 resonant case, one has the next result [18] given in Proposition 3.

Proposition 3. *A necessary condition for the existence of a* 1:1 *resonant double Hopf bifurcation at* $\eta^* = (\eta_1^*, \eta_2^*)$, *with frequency* $\omega^* \neq 0$ *is*

$$\begin{aligned} F_1(\omega^*, (\eta_1^*, \eta_2^*)) &= F_2(\omega^*, (\eta_1^*, \eta_2^*)) = 0, \\ \frac{\partial F_1}{\partial \omega}(\omega^*, (\eta_1^*, \eta_2^*)) &= \frac{\partial F_2}{\partial \omega}(\omega^*, (\eta_1^*, \eta_2^*)) = 0. \end{aligned} \tag{10}$$

The phenomenon of the 1:1 resonant double Hopf bifurcation occurs naturally when one intends to continue the curve of *regular* double Hopf points (*regular* means non-resonant in this context). This singularity has been widely analyzed and it is known that three parameters are necessary to understand its

unfolding (see one recent application in [14]). From now on, consider the three-dimensional parameter space $\eta = (\eta_1, \eta_2, \eta_3)$. Then, the nearby Hopf points to the concerning singularity describe a special surface, called Whitney umbrella [6]. Forthwith, this result is now formalized through the characteristic functions F_1 and F_2 in the frequency setting.

Theorem 1 (1:1 resonant double Hopf bifurcation)**.**
It is supposed that

$$\text{(i)} \quad \begin{cases} F_1 = F_2 = 0, \\ \dfrac{\partial F_1}{\partial \omega} = \dfrac{\partial F_2}{\partial \omega} = 0, \end{cases} \qquad at\ P = P_0 = (\omega^*, \eta^*), \quad where\ \eta^* = (\eta_1^*, \eta_2^*, \eta_3^*),$$

$$\text{(ii)} \quad \frac{\partial^2 F_1}{\partial \omega^2} \neq 0, \quad or \quad \frac{\partial^2 F_2}{\partial \omega^2} \neq 0 \quad at\ P = P_0 \quad and$$

$$\text{(iii)} \quad \left| \frac{\partial (F_1, F_2)}{\partial (\eta_1, \eta_2)} \bigg|_{P=P_0} \right| \neq 0.$$

Then the set of Hopf bifurcation points close to $\eta^* = (\eta_1^*, \eta_2^*, \eta_3^*)$ is defined through a certain surface in the parameter space (η_1, η_2, η_3), which is diffeomorphically equivalent to a Whitney umbrella, whose normal form is:

$$y^2 = zx^2 \Leftrightarrow \begin{cases} x = a, \\ y = ab, \\ z = b^2, \end{cases} \qquad (a, b) \in \mathcal{E}(0) \subset R^2 \tag{11}$$

where $\mathcal{E}(0)$ is a certain neighborhood of $0 \in R^2$.

Proof. This statement is the frequency domain counterpart of the corresponding one proved in [6]. □

Employing the normal form (11), typical sections of a Whitney umbrella close to criticality are shown in Figure 1. These curves result from the intersection between the involved surface and the planes $z = x + y + t$, with $t < 1$. The section with the loop shows in its self-crossing a non-resonant double Hopf bifurcation point, which disappears when $t = 0$, giving place to a cusp curve with the remarkable 1:1 resonant double Hopf singularity.

3. Poincaré–Andronov–Hopf Theorem in the Frequency Domain

The original version of Poincaré–Andronov–Hopf theorem in the frequency domain is stated as follows [20,18]:

It is supposed that

(H1) There is only one eigenvalue $\hat{\lambda}$ of $h(\lambda, \mathrm{i}\omega; \eta_1) = 0$, passing through the critical point $(-1 + \mathrm{i}0)$ when ω varies in $(0, \infty)$ in such a way that there is a change in the stability of the equilibrium solution.

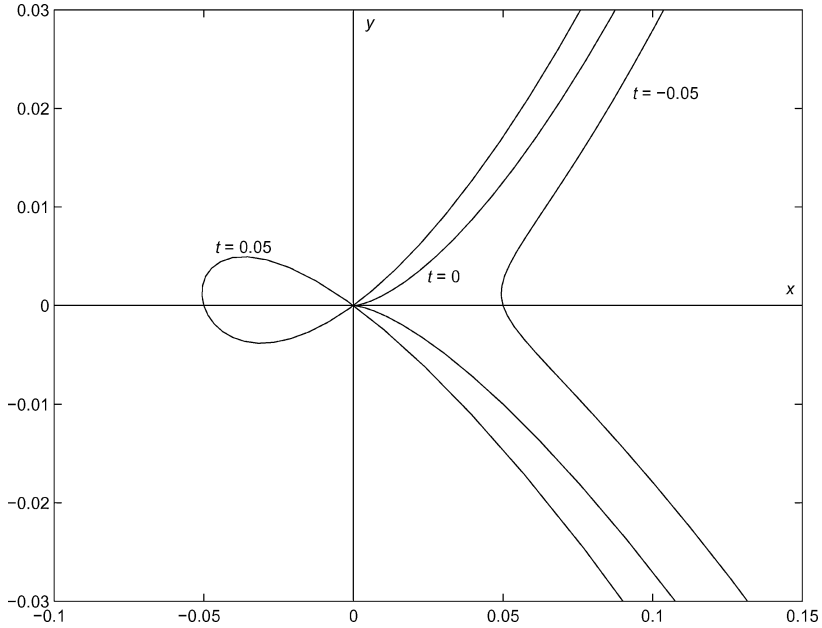

Figure 1. Typical Whitney umbrella's sections close to criticality (using the given normal form (11) with $t = z - (x + y)$).

Moreover, there is only one frequency $\omega_0 \neq 0$ satisfying $h(-1, \mathrm{i}\omega; \eta_1) = 0$ for a given value $\eta_1 = \eta_1^*$, i.e., a resonance condition is avoided, and $\frac{\partial F_1}{\partial \omega}|_{(\omega_0, \eta_1^*)}$, $\frac{\partial F_2}{\partial \omega}|_{(\omega_0, \eta_1^*)}$ are not simultaneously zero,

(H2) The following determinant is nonzero, i.e.,

$$M_1 = \left| \frac{\partial(F_1, F_2)}{\partial(\omega, \eta_1)} \bigg|_{(\omega_0, \eta_1^*)} \right| \neq 0, \tag{12}$$

which is related with the transversality condition of classical formulation, and

(H3) The expression

$$\sigma_1 = -\mathrm{Re}\left(\frac{u^{\mathrm{T}} G(\mathrm{i}\omega_0; \eta_1^*) p_1(\omega_0, \eta_1^*)}{u^{\mathrm{T}} G'(\mathrm{i}\omega_0; \eta_1^*) J(\eta_1^*) v} \right), \tag{13}$$

known as curvature coefficient, that generally allows to analyze the stability of the emerging periodic solution, does not change sign when η_1^* is replaced by a nearby η_1. In the last formula, u^{T} and v are left and right normalized eigenvectors ($u^{\mathrm{T}} v = 1$ and $v^{\mathrm{T}} v = 1$) of the matrix $G(\mathrm{i}\omega; \eta_1) J(\eta_1)$ associated with the eigenvalue $\hat{\lambda}$, $G' = \frac{dG}{ds}$ and p_1 is a complex number whose computation is somewhat complicated since it depends on the information of the second-and third-order partial derivatives of the function $g = [g_1 g_2 \dots g_p]^{\mathrm{T}}$ [18, 20], and

$$\begin{aligned} p_1(\omega, \eta_1) &= QV_{02} + \frac{1}{2}\bar{Q}V_{22} + \frac{1}{8}L\bar{v}, \\ V_{02} &= -\frac{1}{4}H(0; \eta_1)Q\bar{v} \\ V_{22} &= -\frac{1}{4}H(\mathrm{i}2\omega; \eta_1)Qv \end{aligned} \tag{14}$$

where "$\bar{\cdot}$" denotes the complex conjugate, $H(s;\eta_1)=[I+G(s;\eta_1)J(\eta_1)]^{-1}G(s;\eta_1)$ is the so-called closed-loop transfer matrix; the $p\times l$ matrices Q and L are

$$Q=[Q_{jk}]=\left[\sum_{m=1}^{l}\frac{\partial^2 g_j}{\partial y_m\partial y_k}\bigg|_{\tilde{y}}v_m\right] \tag{15}$$

where $v=[v_1 v_2\ldots v_l]^{\mathrm{T}}$, and

$$L=[L_{jk}]=\left[\sum_{m=1}^{l}\sum_{i=1}^{l}\frac{\partial^3 g_j}{\partial y_m\partial y_i\partial y_k}\bigg|_{\tilde{y}}v_m v_i\right] \tag{16}$$

where $j=1,2,\ldots,p, k=1,2,\ldots,l$. All the functions involved in the expression of σ_1 must be evaluated at criticality.

Then, emerging from $\eta_1=\eta_1^*$, there is a branch of periodic solutions whose direction and stability are determined by the values of M_1 and σ_1.

For the determination of the periodic solution, one follows some steps: at first, one considers a fixed value $\tilde{\eta}_1$ next to η_1^* and a first particular estimation for the frequency, $\tilde{\omega}$, the one which comes from the intersection of $\hat{\lambda}=\hat{\lambda}(\omega,\tilde{\eta}_1)$, and the negative real axis, closest to $(-1+\mathrm{i}0)$. Then, taking into account this new pair $(\tilde{\omega},\tilde{\eta}_1)$, one recalculates the eigenvectors u^{T}, v, and the number p_1, adding the computation of the complex number $\xi_1=-u^{\mathrm{T}}G(\mathrm{i}\tilde{\omega};\tilde{\eta}_1)p_1$. Finally, one finds the intersection between the characteristic locus $\hat{\lambda}$ and the so-called *amplitude locus* $L_1=-1+\xi_1\theta^2$, trying to solve a fixed point-like problem. Thereby, accurate approximations of the frequency $\hat{\omega}=\hat{\omega}(\tilde{\eta}_1)$ and the amplitude of the oscillation $\hat{\theta}=\hat{\theta}(\tilde{\eta}_1)$ are attained like in any classical approximation of periodic solution emerging from the Hopf point. Hence, employing harmonic balance of second order results the semi-analytical expression for the approximate output y of system (2) close to the equilibrium $\tilde{y}$, namely

$$y(t)=\tilde{y}+\mathrm{Re}\left(\sum_{k=0}^{2}E_k\exp(\mathrm{i}k\hat{\omega}t)\right) \tag{17}$$

where $E_0=\hat{\theta}^2V_{02}$, $E_1=\hat{\theta}v+\hat{\theta}^3V_{13}=\hat{\theta}V_{11}+\hat{\theta}^3V_{13}$, $E_2=\hat{\theta}^2V_{22}$. The vector V_{13} can be obtained solving the equation

$$P[I+G(\mathrm{i}\hat{\omega};\tilde{\eta}_1)J(\tilde{\eta}_1)]V_{13}=-PG(\mathrm{i}\hat{\omega};\tilde{\eta}_1)p_1, \tag{18}$$

where $P=I-V_{11}V_{11}^{\mathrm{T}}$, under the condition $V_{13}\perp V_{11}$. All the calculations with the nonlinear function g must be evaluated at $\tilde{y}$ for $\eta_1=\tilde{\eta}_1$. Thus, one can reach the solution of (2) in terms of the original state variable x employing (17). This is a brief description of the second-order harmonic balance method which yields an approximate expression for the existing limit cycle.

An improvement of this method has been presented in [21]. To handle approximations of periodic solutions by higher-order formulae, suppose $2q$-th order, one must obtain the coefficients E_k, $0\le k\le 2q$, for an expression like (17). The computation of these numbers is increasingly complicated as long as the accuracy is substantially improved. It is important to point out that the higher-order approximation is still local, a result which is standard for Hopf bifurcation. However,

this higher order approximation will be used to recover the unfolding of the double-Hopf singularity but in the vicinity of "regular" Hopf bifurcation, where the results are quite accurate. To calculate the fourth-order harmonic approximation, one must consider as an initial condition the solution pair obtained at the final stage of the second order case, up to now noted as $(\hat{\omega}, \hat{\theta}) = (\omega_1, \theta_1)$. The main idea is to repeat the above scheme, but in this occasion using a redefined amplitude locus $L_2 = -1 + \xi_1(\omega_1)\theta^2 + \xi_2(\omega_1)\theta^4$ in the fundamental equation (ξ_2 is a complex number of significant tedious computation). The final solution (ω_2, θ_2) will allow to write the coefficients E_k, $0 \leq k \leq 4$, that are involved in the fourth-order harmonic balance approximation. The details about the computation of these coefficients, up to eighth-order, including explicit expressions, can be found in [18]. Using these formulae, the approximation of the periodic solutions up to eight harmonics has been obtained in Section 5.

4. Stability Analysis of Periodic Solutions

It is known that the stability of a periodic solution $\mathbf{X} = \mathbf{X}(t; \tilde{\eta}_1)$, of period T can be studied on a cross-section to the flow of system (1), through the behavior of a fixed point of the associated Poincaré map. Then, the theory of nonlinear discrete-time systems can be applied: one must evaluate the eigenvalues or multipliers (noted as μ_i) of the Jacobian about the fixed point to analyze its stability. Particularly, if all the eigenvalues are placed inside the unit circle (known as the hyperbolicity condition), it can be asserted that the limit cycle is stable. This condition can be violated in three different ways: either a simple positive eigenvalue approaches the unit circle, giving $\mu_1 = 1$, or a simple negative multiplier comes near the unit circle and $\mu_1 = -1$, or a pair of simple complex eigenvalues reaches the unit circle, with $\mu_{1,2} = \exp(\pm \mathrm{i}\gamma_0)$, $0 < \gamma_0 < \pi$, for some value of the bifurcation parameter η_1. These situations give place to fold, transcritical or pitchfork bifurcation for the first situation; flip (period doubling) for the second case and Neimark–Sacker (torus) bifurcations for the crossing of complex eigenvalues.

Due to the difficulty for obtaining an analytical expression of the Poincaré map, the stability analysis is carried out solving the variational equation

$$\dot{z} = D(t)z, \tag{19}$$

where $z \in R^n$, $\dot{z} = \frac{dz}{dt}$ and $D(t) = D_1 f(\mathbf{X}(t; \tilde{\eta}_1); \tilde{\eta}_1) = \frac{\partial f}{\partial x}|_{x=\mathbf{X}(t;\tilde{\eta}_1), \eta_1=\tilde{\eta}_1}$ (observe system (1)), $D(t + T) = D(t)$.

Hence, finding the solution $M = M(t)$ which satisfies $\dot{M} = D(t)M$, $M(0) = I$, where I is the $n \times n$ identity matrix and calculating $M(T)$, one obtains the monodromy matrix of the cycle $\mathbf{X}$. The following result is valid [3].

Theorem 2. *The monodromy matrix $M(T)$ has the eigenvalues $\mu_0 = 1$ and $\{\mu_i\}_{i=1}^{n-1}$ where $\{\mu_i\}_{i=1}^{n-1}$ are the multipliers of the Poincaré map related with the limit cycle* $\mathbf{X}$.

When one of the eigenvalues of $M(T)$ crosses the unit circle, a bifurcation of cycles is established as has been described above. If the crossing happens through a pair of complex conjugate numbers, then Neimark–Sacker or torus bifurcation appears. This singularity is related with the existence of quasi-periodic solutions and forthwith will be the focus of the numerical determination.

5. The Non-Resonant Double Hopf Bifurcation

The phenomenon of non-resonant double Hopf bifurcation takes place at R^n, where $n \geq 4$. It is known that this problem is related with the treatment of a singularity of codimension 2. Thereby, it is necessary to analyze the non-hyperbolic equilibrium points which exist in a neighborhood of (η_1^*, η_2^*) in the parameter space η. Applying normal forms theory [9], several regions where the flow exhibits qualitatively different behaviors can be clearly distinguished [3, 4]. A Hopf bifurcation curve appears in the neighborhood of the point (η_1^*, η_2^*). Its two branches, each one related with one frequency ω_i, $i = 1, 2$, intersect the other while passing through criticality, besides changing its stability in the crossing. Furthermore, these branches divide stability zones for the equilibrium of the system.

At first place, the semi-analytical approximations of periodic solutions, next to the referred curve, have been obtained using harmonic balance of different orders. Their accuracy have been evaluated through the eigenvalues of the monodromy matrix, particularly measuring the error in the computation of the eigenvalue that theoretically should be one, since the analysis has considered that the system is established in a periodic solution [22].

According with very known results, the stability of the periodic branch (in this case arising from Hopf bifurcation) changes when the monodromy matrix has a pair of complex conjugate eigenvalues which crosses the unit circle. This situation is recognized in the context of bifurcation of maps as the Neimark–Sacker bifurcation, which gives place to a secondary Hopf or torus bifurcation, characterized by the appearance of a quasi-periodic solution which can be dense on a two-dimensional (2-D) torus contained in R^3. More specifically, the semi-analytical approximate expression of the limit cycles around the point (η_1^*, η_2^*) is rather accurate because it involves eight harmonics. After employing Floquet theory, the existing curves of secondary Hopf bifurcations have been built. Moreover, the dynamical analysis in the region between these singularity curves and the Hopf curve branches in the parameter space has been carried out. According with these results, the observed transformation of the phase space is outstanding, due to the interactions of two cycles which finally lead to the appearance of the aforementioned quasi-periodic solution.

5.1. Example

It is considered a nonlinear system [4], which models a two RCL coupled circuit as shown in Figure 2(a), with capacitors C_1, C_2, inductors L_1, L_2 and a resistor R.[1] The conductance is a nonlinear element, governed by the following law: $i_G = -\frac{1}{2}v_G + v_G^3$, where i_G and v_G are the current and voltage of the conductance, respectively. Choosing the voltages across the capacitors and the currents in the inductors as the state variables and calling $x = (x_1, x_2, x_3, x_4) = (v_{C_1}, i_{L_1}, v_{C_2}, i_{L_2})$ follows the system

$$\begin{aligned}
\dot{x}_1 &= \frac{1}{2}\eta_1 x_1 + \eta_1 x_2 - \eta_1 x_4 - \eta_1 x_1^3, \\
\dot{x}_2 &= -\frac{\sqrt{2}}{2}x_1, \\
\dot{x}_3 &= (\sqrt{2}+1)x_4, \\
\dot{x}_4 &= (2-\sqrt{2})(x_1 - x_3 - \eta_2 x_4),
\end{aligned} \tag{20}$$

[1] A quite similar problem, but in this case started in wind engineering, has been analyzed in [15] and later studied in [18] with this frequency domain approach but only regarding the stability of the equilibrium solution and the crossings of its Nyquist diagram through criticality.

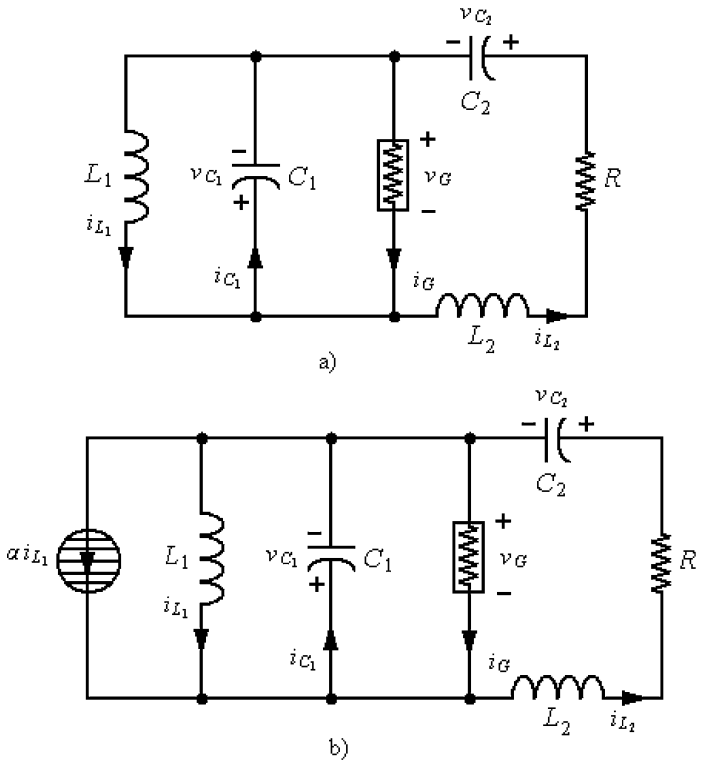

Figure 2. (a) An electrical circuit. (b) Modified electrical circuit.

where $\dot{x}_i = \frac{dx_i}{dt}, i = 1, \ldots, 4,\ \eta_1 = \frac{1}{C_1}$ and $\eta_2 = R$ are considered as two independent bifurcation parameters and $C_2 = \frac{1}{\sqrt{2}+1}, L_1 = \frac{2}{\sqrt{2}}$ and $L_2 = \frac{1}{2-\sqrt{2}}$.

It is easy to see that the unique equilibrium point results $\tilde{x}_i = 0, i = 1, \ldots, 4$. Then, the linearization of the system (20) at the origin gives the following characteristic polynomial:

$$\begin{aligned} P(r) = r^4 &+ \left(2\eta_2 - \eta_2\sqrt{2} - \frac{\eta_1}{2}\right)r^3 \\ &+ \left(-\frac{\eta_1}{2}\sqrt{2} + 2\eta_1 - \eta_1\eta_2 + \frac{\eta_1\eta_2}{2}\sqrt{2} + \sqrt{2}\right)r^2 \\ &+ \left(\eta_1\eta_2\sqrt{2} - \eta_1\eta_2 - \frac{\eta_1}{2}\sqrt{2}\right)r + \eta_1. \end{aligned} \tag{21}$$

This example has been studied in relation with the phenomenon of non-resonant double Hopf bifurcation, under normal forms theory. As long as the analyzed Jacobian has two pairs of imaginary pure eigenvalues, say $\pm i\omega_1, \pm i\omega_2$, where (ω_1/ω_2) is irrational, the coefficients of first and third grade of $P(r)$ must be zero. Thereby

$$\begin{aligned} 2\eta_2 - \eta_2\sqrt{2} - \frac{\eta_1}{2} &= 0, \\ \eta_1\eta_2\sqrt{2} - \eta_1\eta_2 - \frac{\eta_1}{2}\sqrt{2} &= 0, \end{aligned} \tag{22}$$

whose solutions are $\eta_1 = \eta_2 = 0$ (no Hopf bifurcation occurs) and $\eta_1 = 2$, $\eta_2 = 1 + \frac{\sqrt{2}}{2}$. In this last case, the evaluation of the remaining significant coefficients of $P(r)$ gives the system

$$\begin{aligned} \omega_1^2 + \omega_2^2 &= 3, \\ \omega_1^2 \omega_2^2 &= 2, \end{aligned} \tag{23}$$

and follows the unique solution pair $\omega_1 = 1$, $\omega_2 = \sqrt{2}$, if one supposes that $0 < \omega_1 < \omega_2$.

A realization of system (20), like the one described in Section 2, allows to apply all the expounded results in the frequency domain setting. Considering $\dot{x} = (\dot{x}_1, \dot{x}_2, \dot{x}_3, \dot{x}_4)^{\mathrm{T}}$ and the matrices

$$A = \begin{bmatrix} 0 & \eta_1 & 0 & -\eta_1 \\ -\frac{\sqrt{2}}{2} & 0 & 0 & 0 \\ 0 & 0 & 0 & \sqrt{2}+1 \\ 2-\sqrt{2} & 0 & -(2-\sqrt{2}) & -(2-\sqrt{2})\eta_2 \end{bmatrix}, \quad B = \begin{bmatrix} 1 \\ 0 \\ 0 \\ 0 \end{bmatrix} \quad \text{and}$$

$$C = \begin{bmatrix} 1 & 0 & 0 & 0 \end{bmatrix}$$

result

$$\dot{x} = Ax + Bu, \tag{24}$$

where $u = g(y; \eta_1) = -\frac{1}{2}\eta_1 y + \eta_1 y^3$ and $y = -Cx = -x_1$.

Applying Laplace Transform, it is attained the following equilibrium solution:

$$\tilde{y} = -G(0; (\eta_1, \eta_2))g(\tilde{y}; \eta_1), \tag{25}$$

where G is the transfer matrix of the linear part of the feedback formulation of the system (20).[2] In this case, its expression is

$$\begin{aligned} G(s; (\eta_1, \eta_2)) &= C(sI - A)^{-1}B \\ &= \frac{2s(s^2 + (2-\sqrt{2})\eta_2 s + \sqrt{2})}{2s^4 + (4-2\sqrt{2})\eta_2 s^3 + \kappa s^2 + (2\sqrt{2}-2)\eta_1\eta_2 s + 2\eta_1}, \end{aligned} \tag{26}$$

where $\kappa = \kappa(\eta_1) = (4-\sqrt{2})\eta_1 + 2\sqrt{2}$.

Provided that $G(0; (\eta_1, \eta_2)) = 0$ if $\eta_1 \neq 0$ (which will be the case as has been pointed out before), the solution of (25) gives $\tilde{y} = 0$, which is the equilibrium in the frequency domain.

Taking into account Lemma 1, the distinguished eigenvalue $\hat{\lambda}$ can be found solving the equation

$$h(\lambda, s; (\eta_1, \eta_2)) = \det(\lambda - G(s; (\eta_1, \eta_2))J(\eta_1)) = 0, \tag{27}$$

[2] Notice that $g(y; \eta_1)$ can be seen as a feedback block in (24) and then a simple choice of this function would be $g(y; \eta_1) = \eta_1 y^3$. However, this choice is inappropriate since the linearized system in the feedback would cancel out at the equilibrium point. This is the reason to consider the linear part $-\frac{1}{2}\eta_1 y$ in the feedback nonlinear block instead of A.

where $J(\eta_1) = D_1 g(\tilde{y}; \eta_1) = \frac{\partial g}{\partial y}|_{y=\tilde{y}=0} = -\frac{1}{2}\eta_1 + 3\eta_1 y^2|_{y=\tilde{y}=0} = -\frac{1}{2}\eta_1$. This yields directly

$$\begin{aligned}\hat{\lambda} &= G(s; (\eta_1, \eta_2))J(\eta_1) \\ &= -\frac{\eta_1 s(s^2 + (2-\sqrt{2})\eta_2 s + \sqrt{2})}{2s^4 + (4-2\sqrt{2})\eta_2 s^3 + \kappa s^2 + (2\sqrt{2}-2)\eta_1\eta_2 s + 2\eta_1}.\end{aligned} \tag{28}$$

Notice that $G(s; (\eta_1, \eta_2))J(\eta_1) = -1$ is the bifurcation condition in the frequency domain, and then it can be easily converted to the characteristic equation $P(r) = 0$ in time domain, replacing "s" by "r". Moreover,

$$\begin{aligned}\hat{\lambda} &= \hat{\lambda}(\omega; (\eta_1, \eta_2)) = G(\mathrm{i}\omega; (\eta_1, \eta_2))J(\eta_1) \\ &= \frac{-\eta_1\eta_2\omega^2(2-\sqrt{2}) + \mathrm{i}\eta_1\omega(\sqrt{2}-\omega^2)}{-2\omega^4 + \kappa\omega^2 - 2\eta_1 + \mathrm{i}((4-2\sqrt{2})\eta_2\omega^3 - (2\sqrt{2}-2)\eta_1\eta_2\omega)}.\end{aligned} \tag{29}$$

It can be observed in Figure 3, the characteristic eigenlocus $\hat{\lambda}$, when $\eta_1 = 2, \eta_2 = 1 + \frac{\sqrt{2}}{2}$, as the parameter ω varies in $[0, \infty)$. Particularly, the two crossings through $(-1 + \mathrm{i}0)$ succeed when the frequency values $\omega_1 = 1$ and $\omega_2 = \sqrt{2}$ are set.

The next objective is to verify the validity of Propositions 1 and 2 at $\eta^* = (\eta_1^*, \eta_2^*) = (2, 1 + \frac{\sqrt{2}}{2})$. Considering the expression of the critical eigenvalue $\hat{\lambda}$, one can obtain the formulae for the functions F_1 and F_2, defined by (6). Thus, due to (29) one can write

$$\hat{\lambda} = \frac{A_1 + \mathrm{i}A_2}{A_3 + \mathrm{i}A_4} = \frac{A_1A_3 + A_2A_4 + \mathrm{i}(A_2A_3 - A_1A_4)}{A_3^2 + A_4^2}, \tag{30}$$

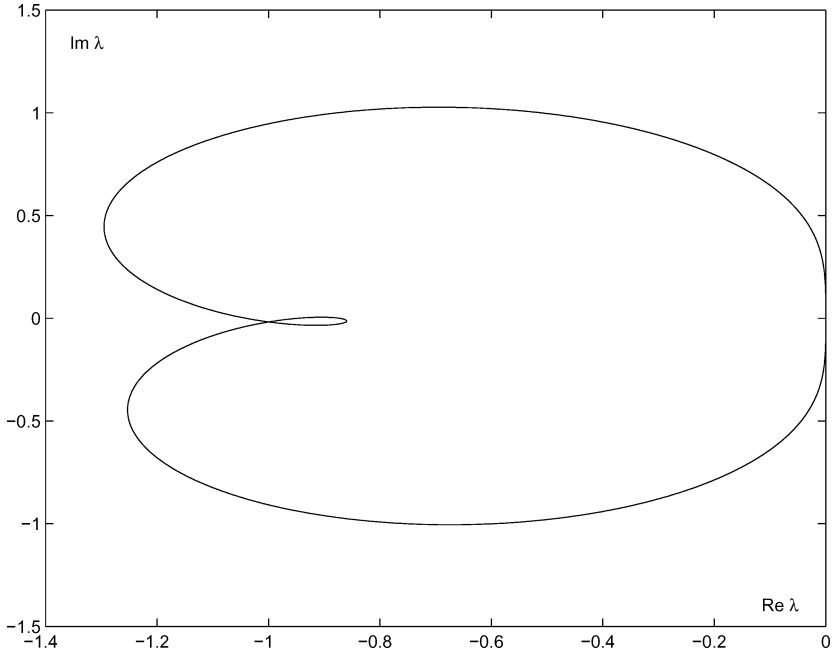

Figure 3. Characteristic eigenlocus or Nyquist diagram for non resonant double Hopf bifurcation.

where

$$\begin{aligned} A_1 &= -\eta_1\eta_2\omega^2(2-\sqrt{2}),\\ A_2 &= \eta_1\omega(\sqrt{2}-\omega^2),\\ A_3 &= -2\omega^4+\kappa\omega^2-2\eta_1,\\ A_4 &= (4-2\sqrt{2})\eta_2\omega^3-(2\sqrt{2}-2)\eta_1\eta_2\omega. \end{aligned} \tag{31}$$

Therefore, it is attained that

$$\begin{aligned} F_1(\omega,(\eta_1,\eta_2)) &= \frac{A_1A_3+A_2A_4}{A_3^2+A_4^2}+1,\\ F_2(\omega,(\eta_1,\eta_2)) &= \frac{A_2A_3-A_1A_4}{A_3^2+A_4^2}. \end{aligned} \tag{32}$$

Stating $\eta^* = (\eta_1^*, \eta_2^*) = (2, 1+\frac{\sqrt{2}}{2})$, for $\omega_1 = 1$ results $F_1 = 0$, $F_2 = 2.8429 \times 10^{-16}$, and for $\omega_2 = \sqrt{2}$ yields $F_1 = -2.2204 \times 10^{-16}$, $F_2 = -1.2319 \times 10^{-15}$, as it is asserted by Proposition 1.

Provided that

$$\left|\frac{\partial(F_1,F_2)}{\partial(\eta_1,\eta_2)}\bigg|_{(\omega_1,\eta^*)}\right| = -0.2071 \neq 0 \quad \text{and} \quad \left|\frac{\partial(F_1,F_2)}{\partial(\eta_1,\eta_2)}\bigg|_{(\omega_2,\eta^*)}\right| = -0.2929 \neq 0, \tag{33}$$

the non-degeneracy condition of the Jacobian is satisfied twice, then follows Proposition 2. Hence, according to the given formulae the tangent vectors t_1, t_2 can be computed, resulting

$$t_1 = (-0.4142, 0.8536) \quad \text{and} \quad t_2 = (-0.2929, -0.8536). \tag{34}$$

Thus, the values $m_1 = -2.0608, m_2 = 2.9142$, which represent the slopes of the tangent lines to the branches of the Hopf curve, H_1 and H_2, at the critical point $\eta^* = (\eta_1^*, \eta_2^*)$, related with the frequencies $\omega_1 = 1$ and $\omega_2 = \sqrt{2}$, respectively, are in agreement with the results expounded in [4]. Furthermore, the continuation of the Hopf curve next to the singularity shown in Figure 4 has been attained employing the corresponding equations (6). This curve has also been checked using LOCBIF [5].

Evaluating the expression of the curvature coefficient σ_1 on the tangent lines (for classical Hopf bifurcation, a negative value of σ_1 means a stable limit cycle), the analysis of stability in each branch can be developed. Therefore, one can observe the changes which happen in the crossing through the singularity. For $\eta_2 > \eta_2^*$, both Hopf branches give place to stable limit cycles, property which is lost at the critical point η^*.

If one adds to the first equation of the system (20), one control function involving an auxiliary parameter η_3, like $\phi = \eta_3 x_2$, results

$$\begin{aligned} \dot{x}_1 &= \frac{1}{2}\eta_1 x_1 + (\eta_1+\eta_3)\,x_2 - \eta_1 x_4 - \eta_1 x_1^3,\\ \dot{x}_2 &= -\frac{\sqrt{2}}{2}x_1,\\ \dot{x}_3 &= (\sqrt{2}+1)x_4,\\ \dot{x}_4 &= (2-\sqrt{2})(x_1 - x_3 - \eta_2 x_4). \end{aligned} \tag{35}$$

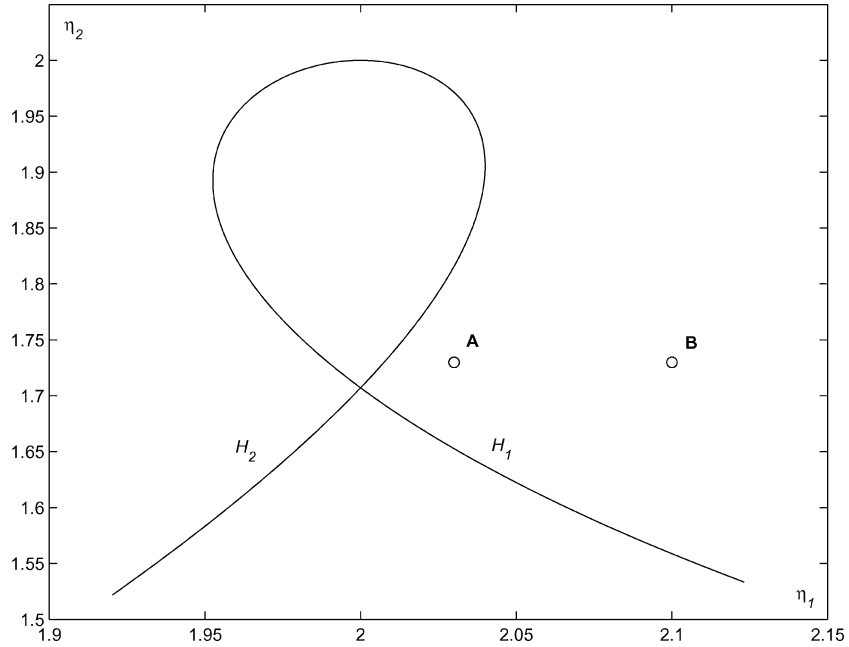

Figure 4. Continuation of Hopf points near non resonant double Hopf bifurcation for the circuit in Figure 2(a) ($\eta_3 = 0$). Points **A** ($\eta_1 = 2.03$, $\eta_2 = 1.73$) and **B** ($\eta_1 = 2.10$, $\eta_2 = 1.73$) are used to estimate the approximation of the stable limit cycle emerging from Hopf bifurcation branch H_2.

This new system has another Hopf degeneracy known as 1:1 resonant double Hopf bifurcation, for the special parameter values $\eta_1^{**} = 4(2-\sqrt{2})$, $\eta_2^{**} = 2$, $\eta_3^{**} = 4\sqrt{2} - 6$. In this case, the critical frequency results $\omega^{**} = \omega_1 = \omega_2 = \sqrt[4]{2}$. Notice that the suggested modification can be implemented adding a current source controlled by the current i_{L_1} in parallel with the inductance L_1. Then, this controlled current source would be of value $\alpha\, i_{L_1}$ where $\alpha = \eta_3/\eta_1$ (see Figure 2(b)). Thus, considering the new proposed system (35) and formulating one realization with

$$A = \begin{bmatrix} 0 & \eta_1+\eta_3 & 0 & -\eta_1 \\ -\frac{\sqrt{2}}{2} & 0 & 0 & 0 \\ 0 & 0 & 0 & \sqrt{2}+1 \\ 2-\sqrt{2} & 0 & -(2-\sqrt{2}) & -(2-\sqrt{2})\eta_2 \end{bmatrix}, \quad B = \begin{bmatrix} 1 \\ 0 \\ 0 \\ 0 \end{bmatrix},$$

$$C = [\,1 \quad 0 \quad 0 \quad 0\,], \quad u = g(y;\eta_1) = -\frac{1}{2}\eta_1 y + \eta_1 y^3 \quad \text{and} \quad y = -Cx = -x_1,$$

first one can find the frequency domain equilibrium, $\tilde{y}_{\mathrm{MOD}} = 0$, then attain the expression of the distinguished eigenvalue

$$\begin{aligned} \hat{\lambda}_{\mathrm{MOD}} &= \hat{\lambda}_{\mathrm{MOD}}(\omega;(\eta_1,\eta_2,\eta_3)) = G(\mathrm{i}\omega;(\eta_1,\eta_2,\eta_3))J(\eta_1) \\ &= \frac{-\eta_1\eta_2\omega^2(2-\sqrt{2}) + \mathrm{i}\eta_1\omega(\sqrt{2}-\omega^2)}{-2\omega^4 + (\kappa(\eta_1)+\sqrt{2}\eta_3)\omega^2 - 2\chi + \mathrm{i}((4-2\sqrt{2})\eta_2\omega^3 - (2\sqrt{2}-2)\chi\eta_2\omega)}, \end{aligned} \tag{36}$$

where $\chi = \eta_1 + \eta_3$, and finally draw its eigenlocus for $(\eta_1^{**}, \eta_2^{**}, \eta_3^{**})$, which looks like Figure 5, noting that the loop in Figure 3 has disappeared at the singularity. Moreover, it is possible to check

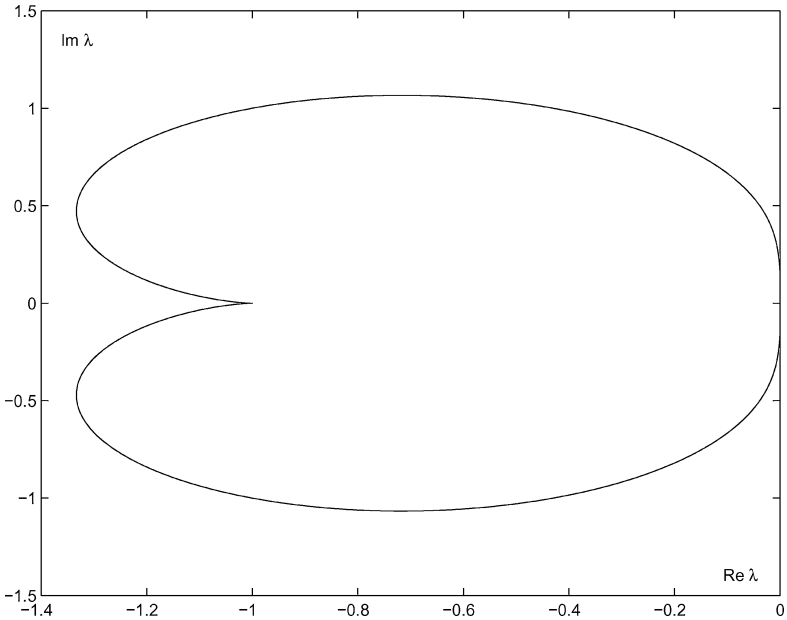

Figure 5. Characteristic eigenlocus for 1:1 resonant double Hopf bifurcation for $(\eta_1^{**}, \eta_2^{**}, \eta_3^{**})$.

Proposition 3 and Theorem 1 and, consequently, affirm that the set of Hopf bifurcation points next to the analyzed Hopf degeneracy point determines a special surface which is described through a parametrization of type $\eta_1 = \eta_1(\omega, \eta_3), \eta_2 = \eta_2(\omega, \eta_3)$, and is diffeomorphic to a Whitney umbrella, in the three-dimensional parameter space (η_1, η_2, η_3). Its remarkable sections obtained using the system (6) should satisfy $F_1(\omega; (\eta_1, \eta_2, \eta_3)) = \mathrm{Re}\{\hat{\lambda}_{\mathrm{MOD}}\} + 1 = 0$ and $F_2(\omega; (\eta_1, \eta_2, \eta_3)) = \mathrm{Im}\{\hat{\lambda}_{\mathrm{MOD}}\} = 0$. Some sections parameterized in η_3 are shown in Figure 6 and are clearly in accordance to Figure 1.

The rest of the development of this example concerns with the computation of higher-order harmonic balance approximations to obtain semi-analytical expressions of limit cycles emerging from regular Hopf bifurcation. Then a calculation of the Floquet multipliers for detecting secondary Hopf (torus) and cyclic fold bifurcations is implemented. According with the last objective, the particular variational system results:

$$\dot{z} = D(t)z, \tag{37}$$

where $D(t)$ has been defined in (19), and for the case of the modified controlled oscillatory circuit example has the following expression:

$$D(t) = \begin{bmatrix} \frac{1}{2}\eta_1 - 3\eta_1 x_1^2 & \eta_1 + \eta_3 & 0 & -\eta_1 \\ -\frac{\sqrt{2}}{2} & 0 & 0 & 0 \\ 0 & 0 & 0 & \sqrt{2}+1 \\ 2-\sqrt{2} & 0 & -(2-\sqrt{2}) & -(2-\sqrt{2})\eta_2 \end{bmatrix}, \tag{38}$$

and $x_1 = x_1(t; (\eta_1, \eta_2, \eta_3))$ is the first component of a generic limit cycle. Thus, the monodromy matrix can be obtained after integrating (37) and then follows the computation of its multipliers.

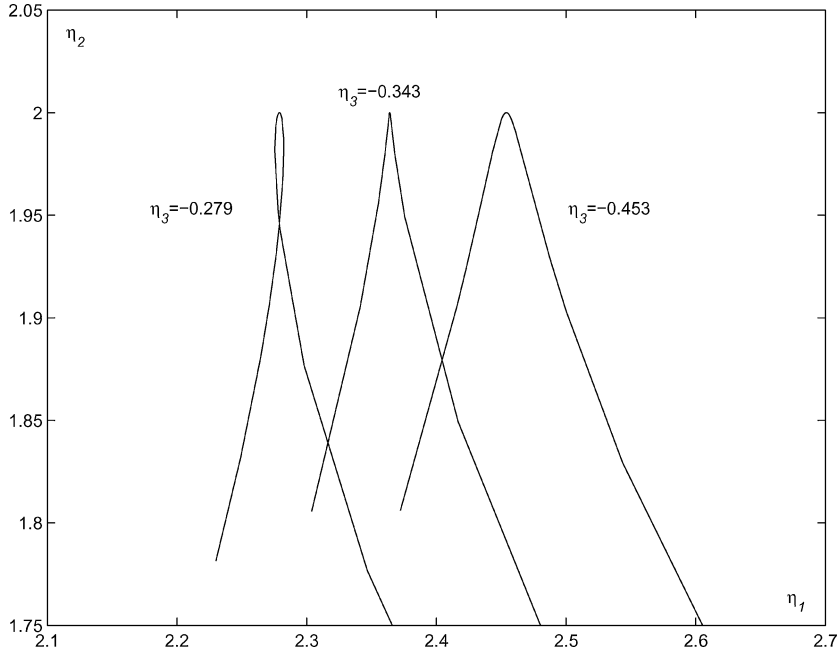

Figure 6. Hopf bifurcation curves close to 1:1 resonant double Hopf bifurcation for the controlled circuit of Figure 2(b).

Consider the particular case: $\eta_1 = 2.03$, $\eta_2 = 1.73$ and $\eta_3 = 0$ (i.e., in the unfolding of the non-resonant double Hopf bifurcation), close to criticality and one stable Hopf branch H_2 (related with the frequency $\omega_2 = \sqrt{2}$), as can be observed in Figure 4 (see the point denoted as **A**). In the frequency setting, the solution has been obtained employing harmonic balance of second- (HB2), fourth- (HB4), sixth- (HB6) and eighth- (HB8) orders. The last approximation has the following expression:

$$\begin{aligned} y(t) = & -0.1605823661\cos(1.442016194t) - 0.0001250750\cos(4.326048582t) \\ & + 0.5365485 \times 10^{-3} \times \sin(4.326048582t) \\ & + 0.2956999525 \times 10^{-5} \times \cos(7.210080970t) \\ & + 0.1075855815 \times 10^{-5} \times \sin(7.210080970t) \\ & + 0.1006251052 \times 10^{-7} \times \cos(10.09411336t) \\ & - 0.1701939794 \times 10^{-7} \times \sin(10.09411336t). \end{aligned} \tag{39}$$

Then, returning to (20), noticing that $y = -x_1$ and taking into account a phase correction, one can directly write the formulae for the original state variables x_1, forthwith x_2, x_4 and finally x_3. Furthermore, one can measure the accuracy of the different approximations, observing the eigenvalue μ_0 of the corresponding monodromy matrix that is closest to one. This multiplier has the following values depending on the order of approximation, $\mu_0(\text{HB2}) = 0.9993508823$, $\mu_0(\text{HB4}) = 1.000044196$, $\mu_0(\text{HB6}) = 1.000000937$, and $\mu_0(\text{HB8}) = 1.000000010$. Then, one can observe that the four approximations give very good results. In the phase space, the corresponding curves are almost identical and besides, in coincidence with the one which comes from the numerical solution. This observation is related fully with the proximity of the selected pair (2.03, 1.73) to the Hopf curve H_2.

Moreover, setting now $\eta_1 = 2.10$, $\eta_2 = 1.73$ and $\eta_3 = 0$ (see point **B** in Figure 4), one can repeat the procedure to obtain the following trivial multiplier for different higher-order expansions $\mu_0(\text{HB2}) =$

0.9965384953, μ_0(HB4) = 1.001688121, μ_0(HB6) = 1.000052091, and μ_0(HB8) = 0.9999974575. Clearly, the accuracy has declined, comparing with the previous case. As can be seen in Figure 7, the phase plane $x_1 - x_2$ shows essentially three curves: one corresponds to the solution obtained by the second-order approximation (HB2), another one which results from the similarity of the solutions coming from the higher harmonic balances (HB4–HB6–HB8) and the last one obtained with LOCBIF [5]. Thus, the last example points out a disadvantage of the proposed method, due to its local character, but it still shows a good approximation, specially the one obtained with HB8 which is of the order of accuracy given by LOCBIF [5].

With the aim of detecting secondary Hopf (or torus) bifurcations in the neighborhood of the non-resonant double Hopf point, the evolution of characteristic multipliers of a generic cycle close to criticality has been analyzed. Suppose that the parameters (η_1, η_2) are set next and below to H_2, close to the singularity (see Figure 4). Then, one builds the semi-analytical expression of the unstable limit cycle with starting frequency close to $\omega_2 = \sqrt{2}$ and analyzes the associated characteristic multipliers. Fixing the value of the parameter η_2 and slightly increasing the initial value η_1, one repeats the procedure. The algorithm stops when a pair of characteristic multipliers crosses the unit circle. Therefore, using HB8, two points, pre- and after- secondary Hopf bifurcation have been detected numerically as shown in Table 1. In the same way, but now starting next and below to H_1, the semi-analytical expression of the unstable limit cycle with frequency close to $\omega_1 = 1$ is computed and its multipliers are presented in Table 2.

Table 1. Detection of two points pre- and after-Neimark–Sacker bifurcation (in the vicinity of H_2), and comparison with LOCBIF.

	HB8	LOCBIF
	$\eta_1 = 1.9912$, $\eta_2 = 1.65$	
μ_0	1.000000024	1.000001
μ_{1-2}	$1.000313\, e^{\pm i2.08777}$	$1.000311 e^{\pm i2.08777}$
μ_3	0.9517772119	0.9517836
	$\eta_1 = 1.9913$, $\eta_2 = 1.65$	
μ_0	1.000000027	1.000001
μ_{1-2}	$0.999949\, e^{\pm i2.08857}$	$0.999943\, e^{\pm i2.08857}$
μ_3	0.9514125900	0.9514149

Table 2. Detection of two points pre- and after-Neimark–Sacker bifurcation (in the vicinity of H_1), and comparison with LOCBIF.

	HB8	LOCBIF
	$\eta_1 = 2.0102$, $\eta_2 = 1.65$	
μ_0	0.9999999927	1.000001
μ_{1-2}	$0.999482\, e^{\pm i3.1106}$	$0.999518\, e^{\pm i3.1107}$
μ_3	0.9464323877	0.946467
	$\eta_1 = 2.0103$, $\eta_2 = 1.65$	
μ_0	0.9999999947	1.000001
μ_{1-2}	$1.000180\, e^{\pm i3.11172}$	$1.000151\, e^{\pm i3.11171}$
μ_3	0.9466623008	0.946675

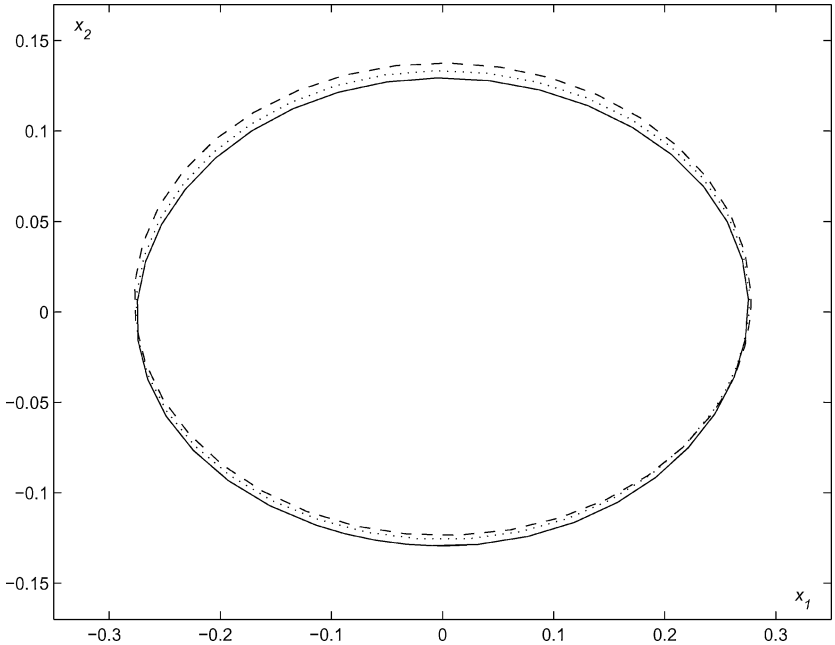

Figure 7. Phase space for $\eta_1 = 2.10$, $\eta_2 = 1.73$ (HB2 (--), harmonic balance approximations higher than second order ($\cdots$), LOCBIF (–)).

This strategy has allowed to build the secondary Hopf bifurcation curves that emerge from the singularity, as can be observed in Figure 8. All the attained results have been contrasted using LOCBIF [5], proving a very auspicious performance of the suggested method. Moreover, computing different higher-order harmonic balances, and trying to measure the accuracy of the approximations, if a condition on the multiplier μ_0 is stated, like $|\mu_0 - 1| < 10^{-4}$, the left secondary Hopf bifurcation branch can be continued up to different η_2 lower limits, namely $\eta_2(\text{HB2}) = 1.67$, $\eta_2(\text{HB4}) = 1.55$, $\eta_2(\text{HB6}) = \eta_2(\text{HB8}) = 1.055$. Comparing the last two cases, it can be mentioned that, computing HB8, the accuracy at criticality is still better, say $|\mu_0 - 1| < 10^{-5}$. On the other hand, repeating this algorithm for the right branch, then one obtains $\eta_2(\text{HB2}) = 1.69$, $\eta_2(\text{HB4}) = 1.53$, $\eta_2(\text{HB6}) = 1.51$ and at last, $\eta_2(\text{HB8}) = 1.33$. This confirms that the frequency domain approach with higher-order balances is suitable for approximating the bifurcation curves of the cycles in the unfolding of the singularity, as stated before.

It is very interesting to analyze the dynamics of the solutions of system (20), when the parameters η_1–η_2 are delimitated between the unstable Hopf curves and the closest Neimark–Sacker curve (see Figure 8). For example, starting below the curve H_1 whose associated frequency is close to $\omega_1 = 1$, two limit cycles coexist: one stable and the other unstable. In Figure 9 the phase portraits of both oscillations have been recovered with the harmonic balance method in two different conditions: one is close to the Neimark–Sacker bifurcation condition (left) and the other to the Hopf bifurcation point (right). As it is clearly noted, these oscillations *interact* when both cycles are close to the Neimark–Sacker curve (see Figure 8). After crossing this curve, the unstable cycle gains stability and an unstable 2-D torus emerges from this singularity. An entirely similar phenomenon appears starting below H_2, when the unstable Hopf curve is now associated to a frequency close to $\omega_2 = \sqrt{2}$.

Let us now analyze the modified system (35), given by Figure 2(b), for $\eta_3 = -0.453$, in which two Hopf degeneracies (HD) of the Whitney umbrella section have appeared (see Figure 6). These

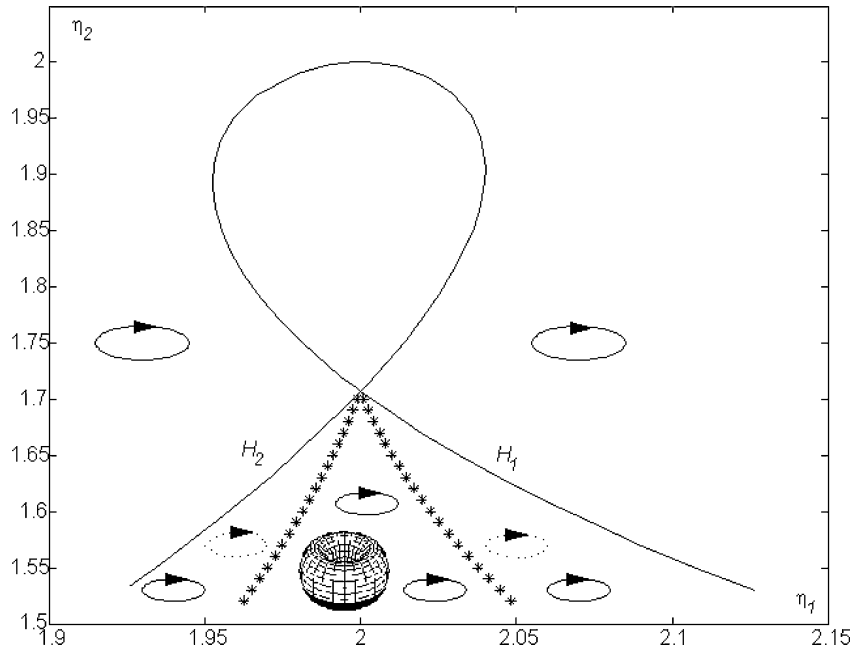

Figure 8. Neimark–Sacker curve (*), in addition to the Hopf curves for the electrical circuit in Figure 2(a). Each region delimitated by Hopf and Neimark–Sacker bifurcation curves has different structures of limit cycles and invariant torus. Circles indicate stable limit cycles, dashed-circles show unstable limit cycles while the torus is unstable. The area without any limit cycle has a stable equilibrium.

degeneracies correspond to the vanishing of the curvature coefficient σ_1, giving a failure of the stability condition. They are located at

$$\begin{aligned} &\mathrm{HD}_1\colon \eta_1 = 2.4222, \quad \eta_2 = 1.924142, \\ &\mathrm{HD}_2\colon \eta_1 = 2.4985, \quad \eta_2 = 1.904058, \end{aligned} \tag{40}$$

and involve the presence of two limit cycles in their neighborhoods [3, 18]. In this particular case, they are both connected with fold bifurcations of cycles (curve F in Figure 10). Following the same technique as above and according to the results exposed in Section 4, the multipliers of the Poincaré map have been considered again, looking for a second eigenvalue (noted as μ_1) which crosses the unit circle along the positive real axis. More precisely, the fold branches emerging from these singularities coalesce and give place to a unique cusp point, as can be observed in Figure 10. For completeness, the Neimark–Sacker bifurcation curve (NS in Figure 10) has also been built. These bifurcation curves have been checked with LOCBIF [5], and comparisons with the results of the frequency domain approach can be seen in Figures 11 and 12, where a quite good agreement is noticed except in the cusp of cyclic fold bifurcations. The appearance of cyclic fold and cyclic cusp bifurcations is in accordance with recent studies [14] concerning the unfoldings of the 1:1 resonant double Hopf bifurcation. It is important to notice that the case 1:1 resonant arises when $\eta_3 = -0.343$ which has not been covered in our study. On the other hand, it is known that a rich qualitative behavior is organized around this degeneracy being Figures 8 and 10 two of the most representative cross-sections of the so-called Whitney umbrella.

Exploring the dynamics of the modified system (35) through Figure 10 and fixing $\eta_1 = 2.45$, the continuation of the existing limit cycles in terms of η_2 is shown in Figure 13, where it is outstanding

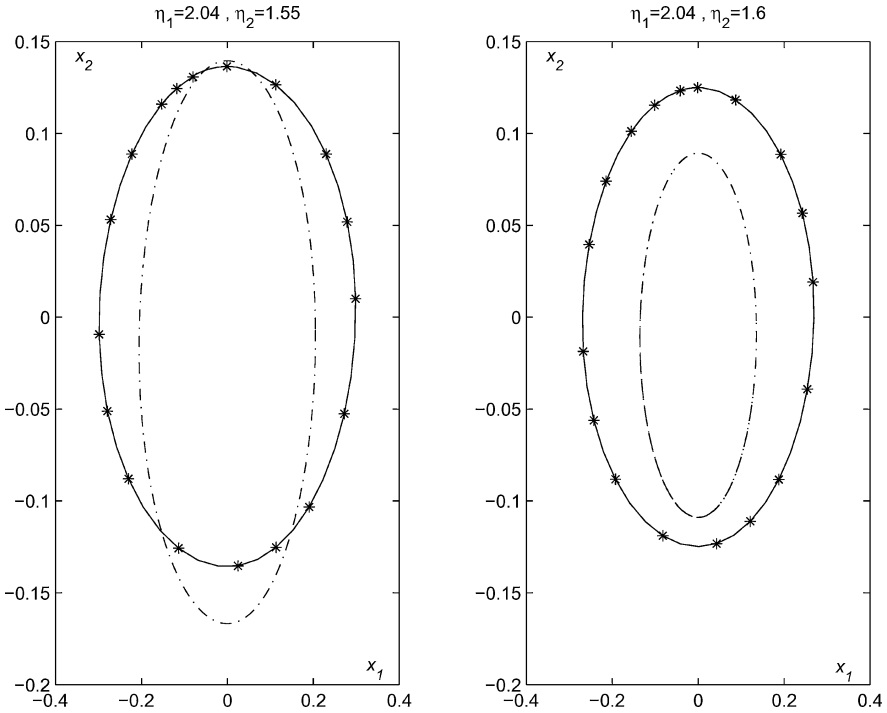

Figure 9. Phase planes in the vicinity of the Neimark–Sacker condition. The stable (–) and unstable (---) cycles are obtained with the frequency domain method, while (*) corresponds to the stable oscillations computed using LOCBIF.

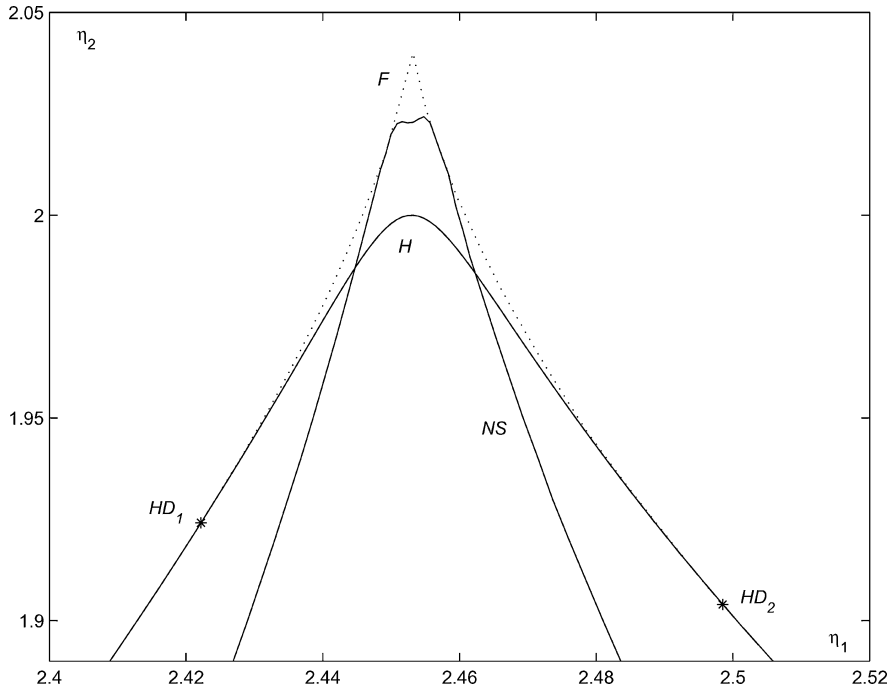

Figure 10. Continuation of fold points (F $(\cdots)$), in addition to the Hopf curve (H) and the Neimark–Sacker curve (NS) for $\eta_3 = -0.453$ by using the frequency domain method. HD_i, $i = 1, 2$, denote degenerate Hopf bifurcations where the first curvature coefficient (or stability index) is zero.

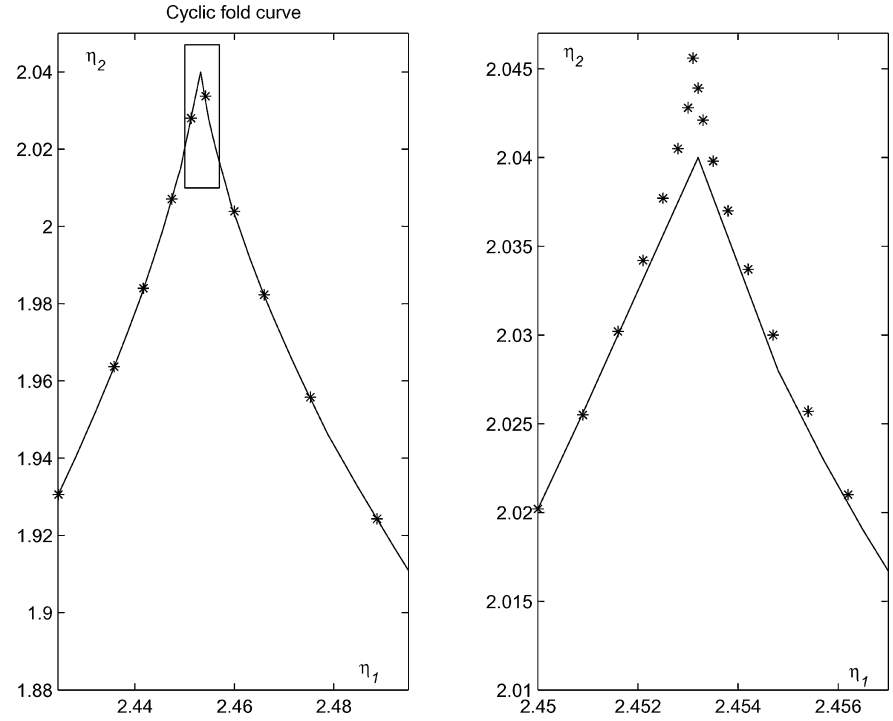

Figure 11. The cyclic fold curve comparison between the frequency domain method (–) and LOCBIF (*) values, for $\eta_3 = -0.453$.

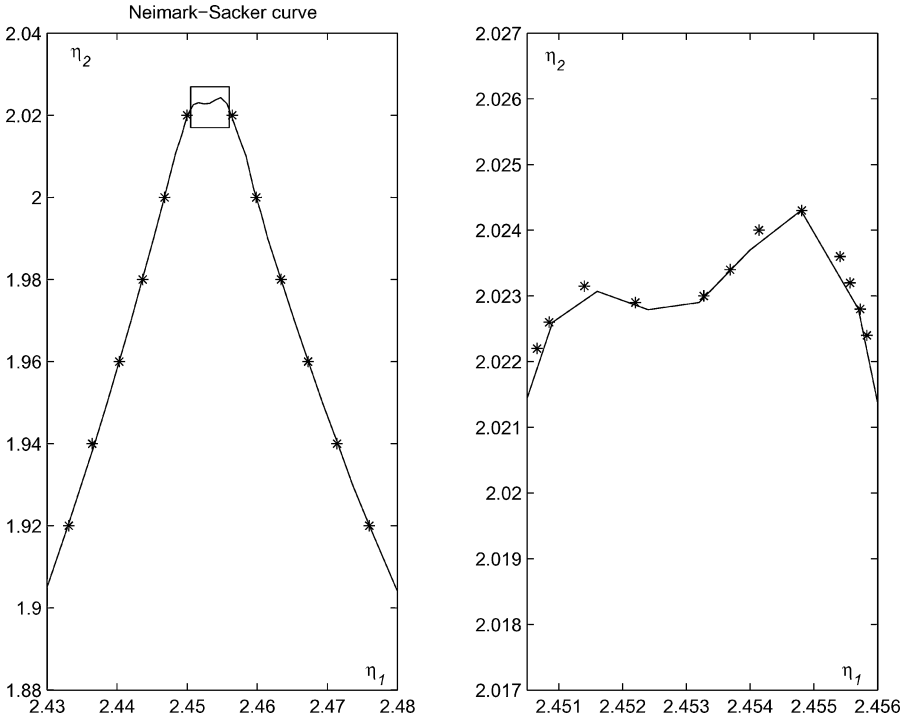

Figure 12. The Neimark–Sacker curve comparison between the frequency domain method (–) and LOCBIF (*) values, for $\eta_3 = -0.453$.

the coexistence up to three limit cycles. Moreover, fixing $\eta_2 = 2.005$ (just over the top of the Whitney umbrella section), the corresponding continuation, now in terms of η_1, is exhibited in Figure 14. It must be pointed out that the last mentioned results have been all compared with those obtained with the softwares LOCBIF [5] and XPP-AUTO [23] and shown in Figures 13 and 14. It is remarkable the

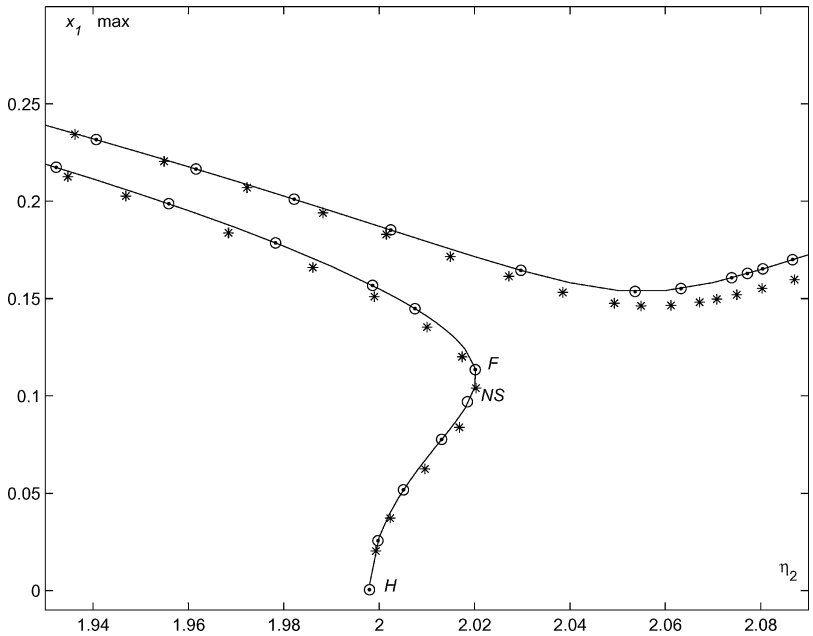

Figure 13. Continuation of the maximum amplitude of limit cycles in terms of η_2 for $\eta_1 = 2.45$ and $\eta_3 = -0.453$ (frequency domain method (–), LOCBIF (*) values, AUTO ($\odot$) values) (fold point (F), Neimark–Sacker point (NS), Hopf point (H)).

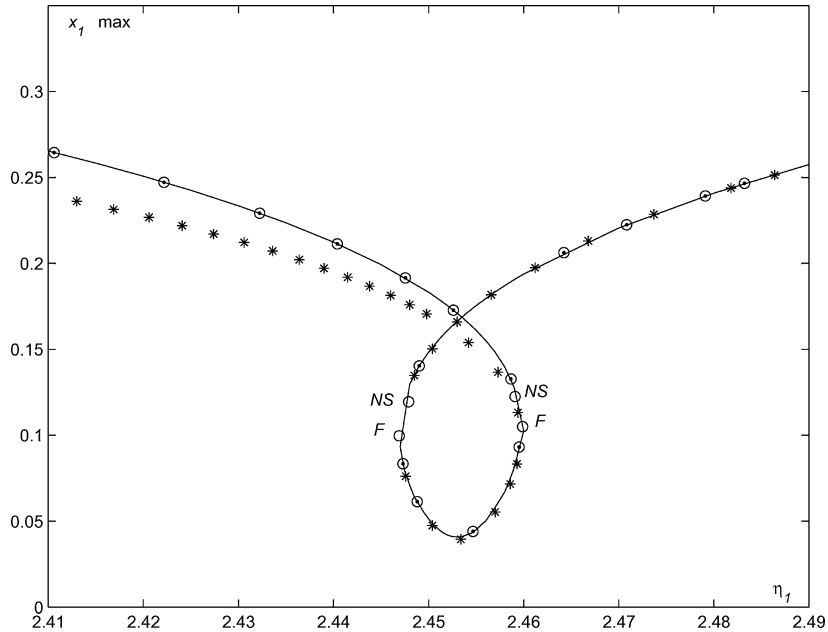

Figure 14. Continuation of the maximum amplitude of limit cycles in terms of η_1 for $\eta_2 = 2.005$ and $\eta_3 = -0.453$ (frequency domain method (–), LOCBIF (*) values, AUTO ($\odot$) values) (fold point (F), Neimark–Sacker point (NS)).

coincidence of results between the frequency domain method and the software XPP-AUTO, specially for predicting maximun amplitudes of limit cycles as well as the location of limit cycles bifurcations (NS and F).

6. Conclusions

This work starts the development of a local dynamical analysis of the double Hopf bifurcation, from the frequency domain point of view. Applying high order harmonic balance and Floquet theory, the unfolding of a non-resonant double Hopf bifurcation has been analyzed. This technique seems to be promising in recovering bifurcations of the cycles in the parameter space emerging from close Hopf (bifurcation) curves, such as in the double Hopf case, fold-Hopf or pitchfork-Hopf bifurcation (also known as Gavrilov–Guckenheimer singularity), and so on. In the future, the possibility of obtaining semi-analytical approximations for quasi-periodic solutions combining harmonic balance techniques as well as related problems of stability and the appearance of n-D torus bifurcations with $n \geq 3$ will be considered.

Acknowledgements

G.R.I. acknowledges the support by Universidad Nacional del Comahue. J.L.M. appreciates the support of CONICET, Universidad Nacional del Sur and ANPCyT (PICT-11-12524). The authors are grateful to the reviewers and Editor for their constructive comments and suggestions, and specially for drawing the attention to reference [14]. Both authors also appreciate the help of Diego Alonso who obtained the results with XPP-AUTO for Figures 13 and 14.

References

1. Hale, J. and Koçak, H., *Dynamics and Bifurcations*, Springer-Verlag, New York, 1991.
2. Guckenheimer, J. and Holmes, P., *Nonlinear Oscillations, Dynamical Systems and Bifurcations of Vector Fields*, Springer-Verlag, New York (fourth printing), 1993.
3. Kuznetsov, Y. A., *Elements of Applied Bifurcation Theory*, Springer-Verlag, New York, 1995.
4. Yu, P., 'Analysis on double Hopf bifurcation using computer algebra with the aid of multiple scales', *Nonlinear Dynamics* **27**, 2002, 19–53.
5. Khibnik, A., Kuznetsov Y. A., Levitin, V. V., and Nikolaev, E. V., 'Continuation techniques and interactive software for bifurcation analysis of ODE's and iterated maps', *Physica D* **62**, 1993, 360–371.
6. Govaerts, W. J. F., Guckenheimer, J., and Khibnik, A., 'Defining functions for multiple Hopf bifurcations', *SIAM Journal of Numerical Analysis* **34**(3), 1997, 1269–1288.
7. Luongo, A. and Paolone, A., 'Perturbation methods for bifurcation analysis from multiple nonresonant complex eigenvalues', *Nonlinear Dynamics* **14**, 1997, 193–210.
8. Nayfeh, A. H., *Perturbation Methods*, Wiley, New York, 1973.
9. Nayfeh, A. H., *Method of Normal Forms*, Wiley, New York, 1993.
10. Torrini, G., Genesio, R., and Tesi, A., 'On the computation of characteristics multipliers for predicting limit cycle bifurcations', *Chaos, Solitons & Fractals* **9**(1/2), 1998, 121–133.
11. Thompson, J. M. T. and Stewart, H. B., *Nonlinear Dynamics and Chaos* Wiley, Chichester, U.K., 1986.
12. Kim, Y.-B., 'Quasi periodic response and stability analysis for non-linear systems: A general approach', *Journal of Sound and Vibration* **192**(4), 1996, 821–833.
13. Gattulli, V., Di Fabio, F., and Luongo, A., 'Simple and double Hopf bifurcations in aeroelastic oscillators with tuned mass dampers', *Journal of The Franklin Institute* **338**, 2001, 187–201.
14. Gattulli, V., Di Fabio, F., and Luongo, A., 'One to one resonant double Hopf bifurcation in aeroelastic oscillators with tuned mass dampers', *Journal of Sound and Vibration* **262**(2), 2003, 201–217.

15. Poore, A. B. and Al-Rawi, A., 'Some applicable Hopf bifurcation formulas and an application in wind engineering', *Annals New York Academy of Sciences* **316**, 1979, 590–604.
16. Ge, Z., Yang, H., Chen, H.-H., and Chen, H.-K., 'Regular and chaotic dynamics of a rotational machine with a centrifugal governor', *International Journal of Engineering Science* **37**, 1999, 921–943.
17. MacFarlane, A. and Postlethwaite, I., 'The generalized Nyquist stability criterion and multivariable root loci', *International Journal of Control* **25**, 1977, 81–127.
18. Moiola, J. and Chen, G., *Hopf Bifurcation Analysis – a Frequency Domain Approach*, Series A, Vol. 21, World Scientific, Singapore, 1996.
19. Itovich, G. and Moiola, J., 'Characterization of static bifurcations in the frequency domain', *International Journal of Bifurcation and Chaos* **11**(3), 2001, 677–688.
20. Mees, A. I. and Chua, L., 'The Hopf bifurcation theorem and its applications to nonlinear oscillations in circuits and systems', *IEEE Transactions on Circuits and Systems* **26**(4), 1979, 235–254.
21. Mees, A. I., *Dynamics of Feedback Systems*, Wiley, Chichester, U.K., 1981.
22. Seydel, R., *Practical Bifurcation and Stability Analysis*, Springer-Verlag, New York, 1994.
23. Ermentrout, B., 'XPPAUT5.0 – the differential equation tool' (available at: www.math.pitt.edu/∼bard/xpp/xpp.html), University of Pittsburg, Pittsburg, Pennsylvania, 2001.